© 2022. Published by The Company of Biologists Ltd | Journal of Experimental Biology (2022) 225, jeb243163. doi:10.1242/jeb.243163

RESEARCH ARTICLE

How octopus arm muscle contractile properties and anatomical organization contribute to arm functional specialization

Letizia Zullo[1,2,*,‡], Alessio Di Clemente[1,3,*] and Federica Maiole[1,3]

ABSTRACT

Octopus arms are highly flexible structures capable of complex motions and are used in a wide repertoire of behaviors. Movements are generated by the coordinated summation of innervation signals to packed arrays of muscles oriented in different directions and moving based on their anatomical relationships. In this study, we investigated the interplay between muscle biomechanics and anatomical organization in the *Octopus vulgaris* arm to elucidate their role in different arm movements. We performed isometric and isotonic force measurements on isolated longitudinal and transverse arm muscles and showed that longitudinal muscles have a higher rate of activation and relaxation, lower twitch-to-tetanus ratio and lower passive tension than transverse muscles, thus prompting their use as faster and slower muscles, respectively. This points to the use of longitudinal muscles in more graded responses, such as those involved in precise actions, and transverse muscles in intense and sustained actions, such as motion stabilization and posture maintenance. Once activated, the arm muscles exert forces that cause deformations of the entire arm, which are determined by the amount, location, properties and orientation of their fibers. Here, we show that, although continuous, the arm manifests a certain degree of morphological specialization, where the arm muscles have a different aspect ratio along the arm. This possibly supports the functional specialization of arm portions observed in various motions, such as fetching and crawling. Hence, the octopus arm as a whole can be seen as a 'reservoir' of possibilities where different types of motion may emerge at the limb level through the co-option of the muscle contractile properties and structural arrangement.

KEY WORDS: Muscle biomechanics, Octopus, Motor control, Invertebrate muscles, Muscular hydrostat, Force–length relationship

INTRODUCTION

In animals, motion is achieved through the coordinated recruitment of specific muscles with an appropriate activation input. In addition, muscle anatomical positioning and the summation of innervation signals allow muscles to move relative to one another and produce limb motion. Hence, movement is determined by a fine interplay between motoneuronal inputs and the organization and type of innervated muscles. In vertebrate animals, the central nervous system activates, based on rigid body coordinates, selected motor brain areas to produce muscle synergies and efficiently accomplish a motor task. Soft-bodied animals have a body unconstrained by rigid skeletal elements, in which motion is obtained through the contraction of muscles against incompressible fluid or tissue, allowing structural deformation or stiffening (Taylor and Kier, 2003). It has been widely demonstrated that the morphological arrangement of muscles may significantly contribute to overall muscle function in a variety of hydrostatic organs (Kier, 2012, 2016; Uyeno and Kier, 2005). *Octopus vulgaris* arms are muscular hydrostats, where flexibility is coupled with a high precision of movement. They can actively elongate, bend and twist through alternate or simultaneous activation of groups of obliquely striated muscles (Kier and Stella, 2007; Zullo et al., 2017). However, the extent to which arm dynamic deformation is dependent on limb-embedded muscular properties and centrally coordinated muscle activation is not yet understood. Central motor control in cephalopods has been functionally investigated in only a limited number of studies. In the octopus, it has been shown that, in the brain's higher motor centers, the absence of motor topographic maps is accompanied by a spatially distributed organization of motor components, allowing for the construction of a large variety of motions (Zullo and Hochner, 2011; Zullo et al., 2009).

In this study, we investigated the extent to which arm motion can emerge at the limb level through the functional and structural characteristics of the muscles comprising the arm. To do so, we studied the interplay between arm muscle physiology and anatomical positioning, and elucidated how these factors may contribute to mechanically diverse arm functions.

We first performed an *in vitro* characterization of the active biomechanical properties of the two main muscle layers of the *Octopus vulgaris* arm bulk, namely the longitudinal and transverse muscles. We investigated their activation properties and force–length relationship to disclose the mechanical principles underlying force and movement production, and to elucidate possible differences in the physiology of muscles occupying the inner to outer arm regions. The octopus arm muscles are functionally similar to vertebrate skeletal muscles. According to the sliding filament hypothesis, the force that muscles generate upon activation is primarily related to their length and is described by the well-known force–length (F–L) curve. This relationship indicates that muscles generate the greatest force at values around their optimal length, often corresponding to the resting length in skeletal muscles, and decreasing forces at both longer and shorter lengths. While skeletal muscles manifest a small range of length variation because of their attachment to rigid structures (the bones) through tendons (for a review, see Burkholder and Lieber, 2001), the octopus arm poses a question in this regard as it is not constrained to a fixed length and undergoes large-scale deformations during motion. This allows arm muscles to theoretically work over different regions of their F–L curve depending on their strain level.

[1]Center for Micro-BioRobotics & Center for Synaptic Neuroscience and Technology (NSYN), Istituto Italiano di Tecnologia, Largo Rosanna Benzi 10, 16132 Genova, Italy. [2]IRCSS, Ospedale Policlinico San Martino, Largo Rosanna Benzi 10, 16132 Genova, Italy. [3]Department of Experimental Medicine, University of Genova, Viale Benedetto XV, 3, 16132 Genova, Italy.
*These authors contributed equally to this work

‡Author for correspondence (letizia.zullo@iit.it)

L.Z., 0000-0003-0503-6312

Received 22 December 2021; Accepted 25 February 2022

Journal of Experimental Biology (2022) 225, jeb243163. doi:10.1242/jeb.243163

List of symbols and abbreviations

AN	axial nerve cord
ASW	artificial sea water
AT	aboral thickness
CSA	cross-sectional area
DT	diagonal thickness
F	force
F_{max}	maximal force
L_0	length at which the maximal isometric force was recorded
L_R	resting length
LA	longitudinal aboral
LL	longitudinal lateral
LO	longitudinal oral
LT	lateral thickness
OME	external oblique muscles
OMI	internal oblique muscles
OMM	median oblique muscles
OT	oral thickness
RM	repeated measures
TA	transverse aboral
TDE	transverse diagonal extension
TL	transverse lateral
TO	transverse oral
V	velocity of shortening
V_{max}	maximum shortening velocity

This feature is particularly relevant in light of the findings of Di Clemente et al. (2021), who showed that hydrostatic pressure is inherently present in the octopus arm and affects both muscle strain and passive biomechanical responses. Moreover, strain variations can also influence the ability of the muscle to produce force, and therefore its function during motion. Hence, muscle fiber contractile properties must be interpreted in light of the muscle architecture and anatomical arrangement.

According to the current literature, the octopus arm has a proximal–distal continuity of muscles, thus seemingly lacking regional diversification. However, evidence of a behavioral 'specialization' of arm portions has been found in various motions such as fetching, crawling, searching and even constrained pulling. In these behaviors, the proximal, medial and distal segments of the arm can be used preferentially or alternatively (Gutnick et al., 2011, 2020; Kennedy et al., 2020; Levy et al., 2015; Richter et al., 2015; Sumbre et al., 2005). However, the principles underlying this functional diversification remain unclear. To elucidate this point, we next performed a detailed investigation of the morphological aspect ratio of transverse and longitudinal muscles along the arm, particularly in the proximal, medial and distal arm regions. We wished to determine whether differences in their morphology underlie the preferential use of distinct arm segments during motion (Kennedy et al., 2020). This would ultimately allow us to infer the specialized, and possibly flexible, role played by the octopus arm hydrostatic muscles during motion.

MATERIALS AND METHODS

Animal treatment

Twenty *Octopus vulgaris* Cuvier 1797 specimens were used in this study. Animals of both sexes (mass 200–300 g) were collected from local anglers on the Ligurian coast of Italy from October to May. Our research conformed to the ethical principles of the three Rs (replacement, reduction and refinement) and of minimizing animal suffering, following Directive 2010/63/EU (Italian D. Lgs. n. 26/2014) and the guidelines from Fiorito et al. (2014, 2015). All experimental procedures were approved by the institutional board and Italian Ministry of Health (authorization no. 465/2017-PR).

After capture, the animals were placed in 80×50×45 cm aquarium tanks filled with artificial seawater (Tropic Marine) and enriched with sand substrate and clay pot dens. The temperature was maintained constant at 17°C, corresponding to the average temperature at the collection site, and continuously circulated through a biological filter system. Oxygenation was ensured using a dedicated aeration system, and all relevant water chemical/physical parameters were checked daily. Animals were allowed to adapt for at least 5 days before the experiments. They were inspected daily and fed shrimp 3 times per week. In this study, the octopus arms were labeled in terms of side (left L or right R from middle to ventral) and position, numbering them in sequence from one to four, following the classical nomenclature (Wells, 1978).

Before the experiments, the animals were anesthetized with 3.5% $MgCl_2$ seawater. A short segment was cut from the proximal, medial and distal portions of one arm per animal (L2, L3 or R2) and kept in aerated artificial sea water (ASW) (NaCl 460 mmol l^{-1}, KCl 10 mmol l^{-1}, $MgCl_2$ 55 mmol l^{-1}, $CaCl_2$ 11 mmol l^{-1}, Hepes 10 mmol l^{-1}, glucose 10 mmol l^{-1}; pH 7.6) at 4°C for both histological and biomechanical procedures.

Histology

For histological procedures, 15 short arm segments were hand cut with a scalpel from the proximal (∼10% of arm length from the base), medial (∼50% of arm length from the base) and distal (∼95% of arm length from the base) regions of five arms from five different animals.

Arm segments were immediately moved to fresh aerated ASW at 4°C. Samples were fixed overnight in 4% paraformaldehyde (PFA) in ASW, cryopreserved in 30% sucrose overnight, embedded in O.C.T. compound (Electron Microscopy Sciences) and sectioned into 20 µm transverse sections with a cryostat microtome (MC5050 Cryostat Microtome, Histoline). Transverse sections were treated with standard Nissl staining and mounted on coverslips using DPX mountant (for details, see Fossati et al., 2011; Maiole et al., 2019). Images of the stained sections were acquired in a bright field using an upright microscope (Nikon Eclipse N*i*) and processed using ImageJ software.

The following morphological measurements were collected [when possible, standard nomenclature following Kier and Stella (2007) was used]: the diagonal thickness of the arm (DT), measured as the distance between the axial nerve cord (AN) and the median oblique muscles (OMM); the transverse muscle diagonal extension (TDE), measured as the distance between the AN and the apex of the transverse muscle 'flag' along the DT (see Fig. S1 for details); aboral distance (aboral thickness, AT) between the AN and external oblique muscle layer (OME); oral distance (oral thickness, OT) between the AN and OME muscle layer; lateral distance (lateral thickness, LT) between the AN and OME muscle layer; and thickness of the longitudinal aboral and oral muscles (LA and LO, respectively); transverse aboral and oral muscles (TA and TO, respectively); transverse lateral muscles (TL); longitudinal lateral muscles (LL); internal oblique muscles (OMI); and OMM (see Fig. 1A for a comprehensive description).

Muscle biomechanics

General procedure

Forty-two whole-arm segments from 15 different animals were hand-cut with a scalpel from one arm proximal–medial portion and immediately moved to fresh aerated ASW. Forty arm muscle strips

Journal of Experimental Biology (2022) 225, jeb243163. doi:10.1242/jeb.243163

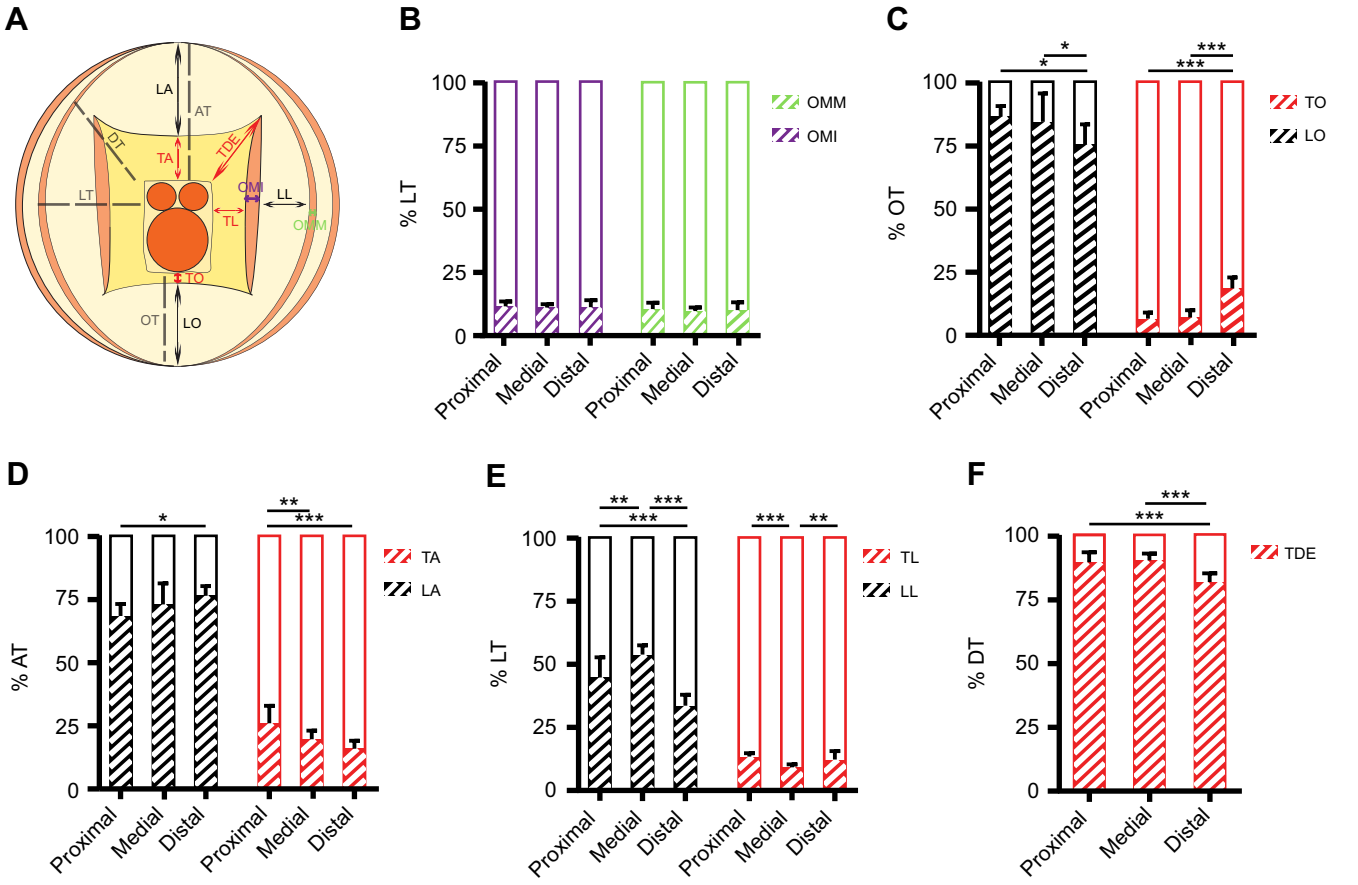

Fig. 1. Muscle aspect ratio along the arm. (A) Schematic representation of an arm transverse section with reference to the measurements obtained: DT, diagonal thickness; TDE, transverse diagonal extension; OT, oral thickness; LO, longitudinal oral; TO, transverse oral; AT, aboral thickness; LA, longitudinal aboral; TA, transverse aboral; LT, lateral thickness; LL, longitudinal lateral; TL, transverse lateral; OMM, median oblique muscles; OMI, inner oblique muscles. Bars show means±s.d. (B) Relative LT of OMI (n=10 proximal, n=10 medial, n=10 distal; one-way ANOVA with Šidák's *post hoc* test, P>0.05) and OMM muscles (n=12 proximal, n=12 medial, n=12 distal; one-way ANOVA with Šidák's *post hoc* test, P>0.05). (C) Relative OT of LO (n=8 proximal, n=12 medial, n=10 distal; one-way ANOVA with Šidák's *post hoc* test, *P<0.05) and TO muscles (n=11 proximal, n=14 medial, n=13 distal; one-way ANOVA with Šidák's *post hoc* test, ***P<0.001). (D) Relative AT of LA (n=9 proximal, n=14 medial, n=14 distal; one-way ANOVA with Šidák's *post hoc* test, *P<0.05) and TA muscles (n=10 proximal, n=14 medial, n=14 distal; one-way ANOVA with Šidák's *post hoc* test, ***P<0.001, **P<0.01). (E) Relative LT of the LL (n=10 proximal, n=11 medial, n=11 distal; one-way ANOVA with Šidák's *post hoc* test, ***P<0.001, **P<0.01) and TL muscles (n=13 proximal, n=12 medial, n=13 distal; one-way ANOVA with Šidák's *post hoc* test, ***P<0.001, **P<0.01). (F) Relative DT of the TDE (n=8 proximal, n=7 medial, n=10 distal; one-way ANOVA with Šidák's *post hoc* test, ***P<0.001).

(length ∼2–5 mm, width ∼1–3 mm, height ∼0.5–1.5 mm), either longitudinal or transverse, were then dissected from the aboral side of the whole-arm samples. To dissect the longitudinal muscles, the epidermis and dermal connective tissue were removed, together with the circumferential and oblique muscle layers. Then, a strip of longitudinal muscle was cut out following the proximo-distal axis. To dissect the transverse muscles, a thin transverse arm slice was cut, and a rectangular strip of the transverse muscle was isolated following a latero-lateral axis.

At the end of each experimental session, samples were collected and treated for histological procedures as described above. The stained sections were used to estimate the percentage of orthogonal fibers in each sample.

The muscle strips were immediately mounted in the recording chamber of a dual-mode lever arm system (ASI 300C-LR, Aurora Scientific Instruments) equipped with stimulating bath electrodes. The samples were attached to a micrometer block on one end and to a lever arm on the other using suture threads (silk suture threads 5/0, Ethicon Inc., code: K880H) and tightened with double square knots. The recording chamber was continuously perfused with oxygenated ASW at ∼16°C using a peristaltic pump (SJ-1220, Atto Co.). This temperature was in the range of the aquarium tanks in which the animals were maintained and was similar to that of the seawater at the collection site. The muscles were allowed to rest for approximately 10 min in the recording chamber prior to the experiment. Particular care was taken to ensure that the perfusion flux did not induce noise in force recordings. The recordings were digitized and analyzed using a LabVIEW-based data acquisition and analysis system (ASI 604A and 605A, Aurora Scientific Instruments). Data were acquired at a sampling frequency of 10 kHz and filtered using a low-pass filter at 3.3 kHz. At the beginning of the experiment, the resting length (L_R) of the muscle strip was adjusted until a transient passive force was apparent, and it was measured using an electronic caliper as the distance between the knots. According to current practice (Kier and Curtin, 2002; Milligan et al., 1997), the stimulus strength–twitch response was determined at the beginning of the experiment for each muscle strip (10 ms stimuli, 60 s interval between successive stimulations). It is worth noting that similar to that observed by Thompson et al. (2014), supramaximal stimulation consistently caused a decrease in the force response; therefore, at the end of the test, we adjusted the stimulus strength to the level employed to reach the maximum force

Journal of Experimental Biology (2022) 225, jeb243163. doi:10.1242/jeb.243163

(Thompson et al., 2014). In our experiments, this corresponded mostly to a value of ∼900 mA (Fig. 2). Preparations that did not reach maximal stimulation were discarded.

Muscle L_0, defined as the length at which the maximal isometric force (F_0) was recorded, was determined for each sample. During the experimental session, the vitality of the preparation was assessed using isometric contractions at L_0. We set a threshold of 10% maximum force decrease to terminate the experimental session and to exclude data from further analysis.

At the end of the experiment, the height (h) and width (w) of the transverse and longitudinal muscle strips were measured at rest using an electronic caliper under a dissection microscope. The cross-sectional area (CSA) of the samples was calculated assuming that they had a parallelepiped shape (for details, see Di Clemente et al. 2021).

Isometric twitch contraction dynamics

Twelve samples from four different animals were used to characterize transverse and longitudinal twitch contraction dynamics. Muscle strips were stimulated with a single current pulse (10 ms) step stimulation, with the length fixed at L_0. The force–time traces were analyzed offline to obtain the time to peak tension and half-relaxation time of each sample. Interestingly, in some samples, we observed after-contraction during the early relaxation phase (Fig. S2 shows an exemplary trace). This interesting phenomenon deserves further investigation. However, in this context, it could influence the calculation of the half-relaxation time and traces manifesting after-contraction were excluded from the analysis of the relaxation kinetics.

Force–length

Ten samples from four animals were used in this experiment. The force–length relationship was investigated using brief tetanic stimulations (50 Hz, 100 ms, 10 ms pulse duration) under static strain conditions. Sequential mechanical strain ranging from 1% to 70% of muscle L_R was tested. Muscle strips were lengthened to the desired length using a 2 s long ramp. The preparations were allowed to rest for 20 s and then stimulated (Fig. S3). The resulting force–time traces were analyzed offline using a custom-written MATLAB algorithm to obtain the passive and active components of the force generated by the muscle. Length data were normalized to the optimal muscle length (L_0), and both passive and active components were normalized to sample F_0.

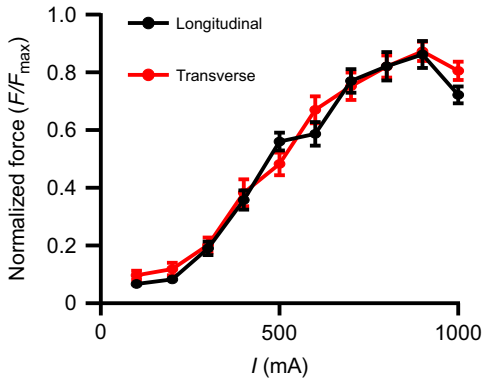

Fig. 2. Stimulus strength–twitch response of the longitudinal and transverse muscles. Normalized force data are presented as means±s.e.m. (n=15 for both experimental groups).

Force–frequency

The force–frequency relationship was investigated under isometric conditions, keeping the muscle length fixed at its L_0. Ten samples from four different animals were tested with 1 s train stimulation (from 1 to 50 Hz, 10 ms pulse duration, 300 s intervals between successive stimulations), as in most cases, shorter durations did not allow samples to reach the maximum plateau force. The peak force generated at each tested frequency was measured offline and used to establish the force–frequency curve. Forces developed at 50 Hz were used to estimate the muscle maximum tetanic tension. To allow comparisons between different samples, the data were normalized to the maximal isometric force developed by each muscle strip.

Force–velocity

The force–velocity relationship was investigated using an isotonic protocol on 10 samples from three different animals. The F_0 of each sample was first determined under isometric conditions with brief tetanic stimulations (50 Hz, 100 ms and 10 ms pulse width) with a fixed length of L_0. The lever arm was then switched to force–clamp mode with imposed loads ranging from 10% to 90% of the sample F_0. A brief tetanic stimulation (same as above) was delivered at each load with 30 s intervals between different trials. The resulting isotonic shortening (exemplary traces in Fig. S4) was analyzed offline using a custom-written MATLAB algorithm to obtain the shortening velocity, which was normalized for sample L_0.

The force–velocity curves were fitted using Hill's equation in the form expressed in Eqn 1:

$$V = V_{\max} \cdot F_{\max} \frac{F_{\max} - F}{G \cdot F + 1}, \quad (1)$$

where V is the velocity of shortening (L_0 s^{-1}), F is the force during shortening normalized to the maximum isometric force, $V_{\max}$ is the intercept on the velocity axis, $F_{\max}$ is the intercept on the force axis, and G is a constant expressing the curvature. The fitting was performed using the ordinary least squares method and was constrained to have $F_{\max}$=1.

Statistical analysis

Statistical analysis was performed using Prism 8 software (GraphPad Software Inc.) unless otherwise indicated. Data normality was assessed using the Shapiro–Wilk normality test. Comparisons among three or more groups were performed using ordinary one-way ANOVA followed by Tukey's *post hoc* test.

A mixed-effects model was employed to adjust for intra-animal variability when necessary.

RESULTS

Muscle aspect ratio along the arm

Here, the organization of the three main muscle groups of the octopus arm, namely transverse, longitudinal and oblique muscles, was analyzed in the proximal, medial and distal arm segments. The thickness of each muscle group was measured in the oral, aboral and lateral regions.

No significant differences were observed in the median and internal oblique muscle thicknesses (OMM and OMI, respectively) along the arm (Fig. 1B).

In the arm oral portion, the relative contribution of the transverse muscles significantly increased in the distal portion (Fig. 1C, one-way ANOVA with Tukey's *post hoc* test, P<0.001), and that of the longitudinal muscles showed a comparable decrease toward the

Journal of Experimental Biology (2022) 225, jeb243163. doi:10.1242/jeb.243163

distal portion (Fig. 1C, one-way ANOVA with Tukey's *post hoc* test, $P<0.05$).

In the arm aboral portion, the relative thickness of the transverse muscles was high in the proximal and medial regions and decreased significantly towards the distal end (Fig. 1D, one-way ANOVA, $P<0.01$, $P<0.001$), whereas the longitudinal muscles were more abundant in the medial and distal regions of the arm and less abundant in the proximal portions (Fig. 1D, one-way ANOVA, $P<0.05$).

In the lateral portion of the arm, the thickness of the transverse muscles was comparable in the proximal and distal portions of the arm, but was significantly lower in the medial arm. Conversely, the longitudinal muscles were significantly more abundant in the medial portion, with a decrease in relative thickness more pronounced in the distal part (Fig. 1E, one-way ANOVA, $P>0.5$).

Transverse muscles occupy the inner portion of the arm, surrounding the AN, and are organized in a butterfly-like shape with large muscle bundles entering the longitudinal aboral muscles and the longitudinal lateral muscles, and assuming typical 'flag' shapes on the two arm sides. The flags on the aboral side connect to the OMM layer through trabeculae of various lengths, depending on the arm segment (proximal, medial and distal). The extension of the aboral flags was measured as the TDE (Fig. 1A; Fig. S1) along arm DT and was found to be significantly lower in the distal portion of the arm than in the proximal or medial portions (Fig. 1F, one-way ANOVA with Tukey's *post hoc* test, $P<0.001$).

Biomechanics

The contractile properties of transverse and longitudinal muscles were extensively characterized by analyzing: (1) the dynamics of twitch contraction; (2) the force–length relationship; (3) the force–frequency relationship; and (4) the force–velocity relationship.

Twitch contraction dynamics

To investigate twitch contraction dynamics of transverse and longitudinal muscles, we analyzed muscle responses to single pulses of stimulation in isometric conditions with muscle strip length fixed at their L_0. In particular, we compared the time to peak tension and the half-relaxation time of the transverse and longitudinal muscles.

The time to peak tension was significantly different between the two muscles. The average value for longitudinal muscles was 59±15 ms and that for transverse muscles was 107±42 ms (Fig. 3A, mixed-effects model, $P<0.001$). The half-relaxation time was also significantly different, with values of 54±12 ms for the longitudinal muscles and 165±39 ms for the transverse muscles (Fig. 3B, mixed-effects model, $P<0.001$). Overall, these results show that transverse muscles manifest slower twitch contraction dynamics.

Force–length relationship

The capability of the muscle to generate force is highly dependent on its length and is described by the force–length relationship.

Force–length active and passive components from a total of 5 longitudinal and 5 transverse muscle preparations are shown in Fig. 4A,B. Passive and active forces were normalized to F_0 of the samples, plotted against their relative lengths (L/L_0), and fitted with a smoothing spline algorithm (dashed and solid lines in Fig. 4A,B). Both muscles were able to produce significant fractions of their F_0 over a relatively wide range of length (the 'plateau' region of the active force–length relationship in Fig. 4A,B). No significant differences were observed in the relative active force that the two muscles could exert at their L_R (Fig. 4C, mixed-effects model, $P>0.05$). Additionally, no difference was found in their L_0 (expressed as a percentage of the sample L_R), reaching values around 30% of stretch (32±18% in transverse and 26±15% in longitudinal) in both muscle types (Fig. 4D, mixed-effects model, $P>0.05$).

Conversely, the passive forces were remarkably different between the two muscles. In the transverse muscles, the passive forces manifested a higher relative contribution to the total force generated. At L_0, passive forces in longitudinal muscle accounted for 14.65±3.08% of the total sample force while in transverse muscles this value was 38.64±14.14% of the total sample force (Fig. 4E, mixed-effects model, $P<0.001$).

Force–frequency relationship

The force–frequency relationship is a crucial determinant of muscle function. Slow twitching muscles, which need to sustain prolonged periods of activity, tend to produce higher forces at lower stimulation frequencies. Conversely, fast muscles usually require higher stimulation frequencies to reach plateau forces.

Here, we characterized the force–frequency relationship of the transverse and longitudinal muscles by stimulating isolated muscle strips under isometric conditions at their L_0. Representative traces for longitudinal and transverse muscles are shown in Fig. 5A; both muscles reached fusion frequencies between 25 and 50 Hz and

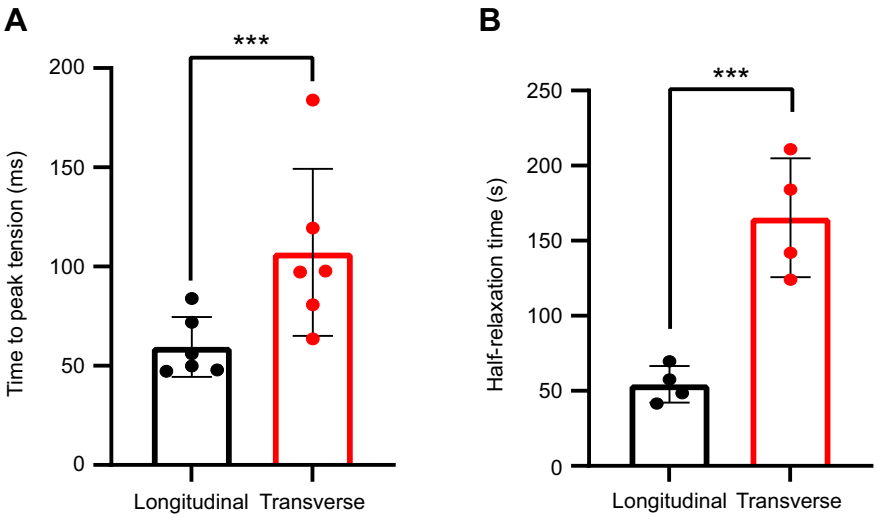

Fig. 3. Twitch contraction dynamics. (A) Time to peak tension (mixed-effects model, ***$P<0.001$, $n=6$ for both experimental groups). (B) Half-relaxation time (mixed-effects model, ***$P<0.001$, $n=4$ for both experimental groups).

Journal of Experimental Biology (2022) 225, jeb243163. doi:10.1242/jeb.243163

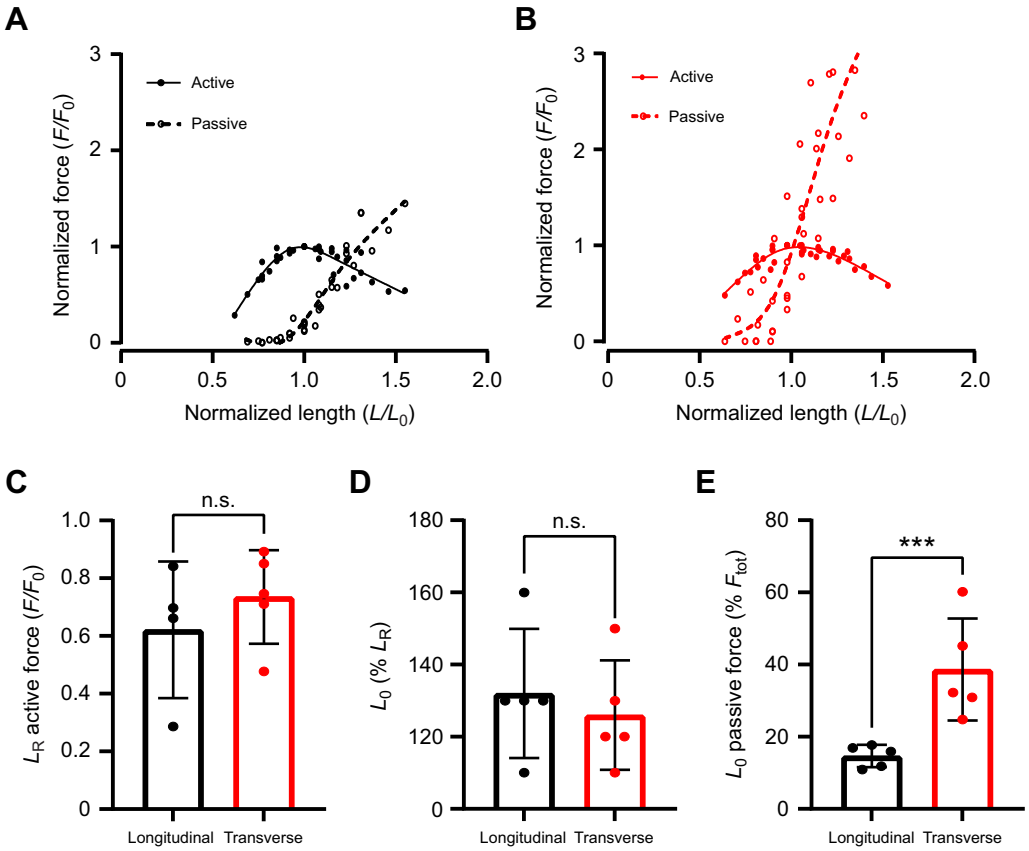

Fig. 4. Force–length relationship. (A) Passive and active force–length relationship of the longitudinal muscles. All data points from n=5 samples are represented. Data were normalized to the sample F_0 and L_0 and fitted with a smoothing spline algorithm (dashed and solid lines). Data fitting is descriptive only. (B) Passive and active force–length relationship of the transverse muscles. All data points from n=5 samples are presented. Data were normalized to the sample F_0 and L_0 and fitted with a smoothing spline algorithm (dashed and solid lines). Data fitting is descriptive only. (C) Relative force (F_R) of the longitudinal and transverse muscles at their resting length (L_R) expressed as a fraction of sample F_0. No significant differences were found between the two muscles (mixed-effects model, P>0.05, n=4 longitudinal, n=5 transverse). Bars show means±s.d. (D) Longitudinal and transverse muscle strip L_0 expressed as a percentage of their L_R. No significant differences were found between the two muscles (mixed-effects model, P>0.05, n=5 for both experimental groups). Bars show means±s.d. (E) Passive contribution to the total force (F_{tot}) developed by the longitudinal and transverse muscle strips at L_0. The transverse muscles showed a significantly higher contribution of passive forces compared with the longitudinal muscles (mixed-effects model, ***P<0.001, n=5 for both experimental groups). Bars show means±s.d.

limited variation of forces occurred at frequencies around 50 Hz. The force–frequency relationship of transverse and longitudinal muscles was found to be significantly different (Fig. 5B, mixed-effects model, P<0.01). Specifically, transverse muscle force increased more steeply at lower frequencies of stimulation. This might underlie a possible difference in the physiology of the arm muscles, with transverse muscle manifesting slower characteristics.

We also measured the twitch to tetanus ratio, which, as expected, was significantly higher in transverse muscles (Fig. 5C, mixed-effects model, P<0.001). This last parameter also depends on several properties of the muscle, including the structural properties of the motor unit, such as the number of fibers composing each motor unit, fiber dimensions and calcium dynamics. While the first parameter is yet to be defined, no evidence has been reported so far on the possible differences in fiber dimension and calcium dynamics in the octopus arm muscles.

The maximal tetanic tension generated by the two muscles at 50 Hz was also different, with mean values of 106.9±22.69 mN mm^{-2} for longitudinal muscles and 56.77±23.22 mN mm^{-2} for transverse muscles. It is worth noting that these values are likely to underestimate actual values. As mentioned above, our preparations incorporate fibers oriented orthogonally to the main force vector (that were not less than 17% in longitudinal muscles and not less than 21% in transverse muscles) that did not contribute to the measured tension. Additionally, transverse muscle fibers are arranged in many directions and, therefore, do not equally contribute to the measured force. Hence, these force values must be taken cautiously, and additional experiments on single fibers are required to obtain a more realistic estimation of the arm muscle fiber forces.

Force–velocity relationship

The force–velocity relationship of transverse and longitudinal muscles was investigated under isotonic conditions imposing loads ranging from 10% to 90% of the maximal isometric force (F_0) of the sample (see Materials and Methods).

Data were normalized to sample L_0, averaged, plotted, and fitted using Hill's equation to extrapolate V_{max} (Fig. 6). The two curves proved to be significantly different, with longitudinal muscles showing higher shortening velocities (Fig. 6, mixed-effects model, P<0.001).

The extrapolated V_{max} was also significantly different between the two muscle types (extra sum-of-squares F-test, P<0.001), with a best-fit value of 0.913 L_0 s^{-1} for longitudinal muscles (95% confidence

Journal of Experimental Biology (2022) 225, jeb243163. doi:10.1242/jeb.243163

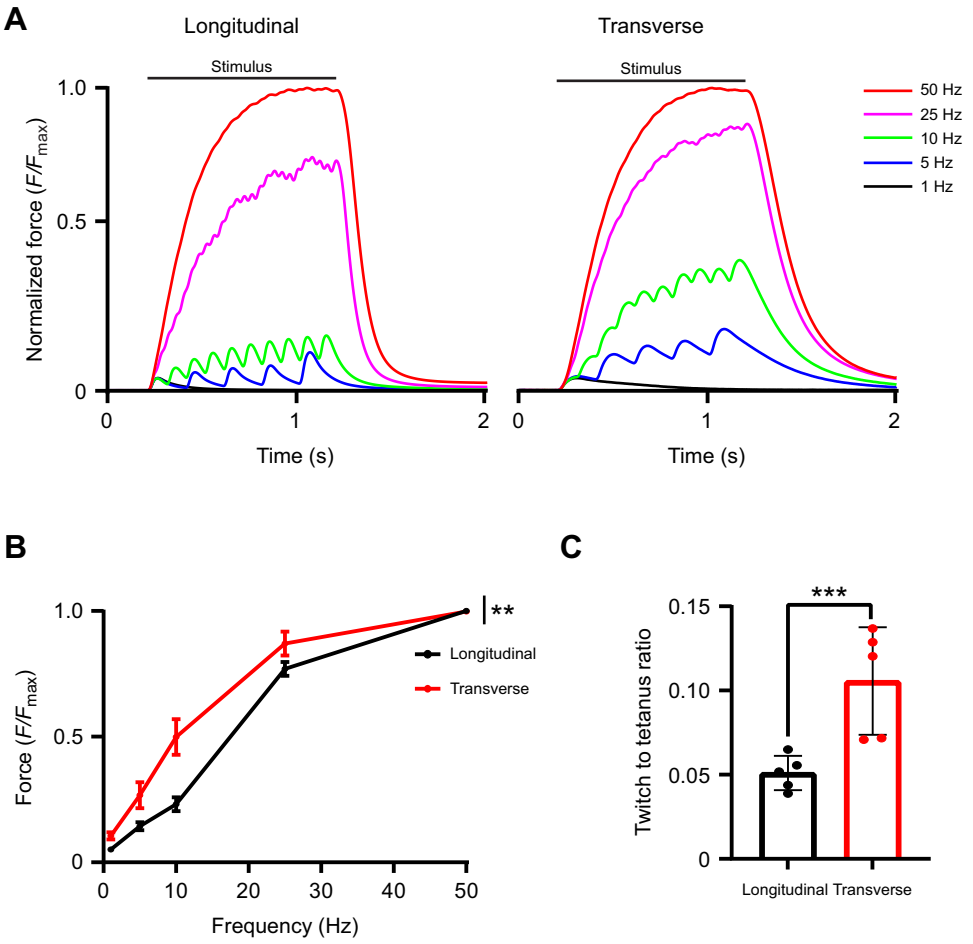

Fig. 5. Force–frequency relationship. (A) Representative force–time traces from one longitudinal (left) and one transverse (right) sample normalized to their maximal isometric force. Stimulus duration is indicated. (B) Average force–frequency curve of transverse and longitudinal muscles. Data are represented as means±s.e.m. The transverse muscles were able to exert higher fractions of their maximal forces at a lower frequency of stimulation (mixed-effects model, $^{**}P<0.01$, $n=5$ for both experimental groups). (C) Twitch to tetanus ratio was significantly higher in transverse muscles (mixed-effects model, $^{***}P<0.001$, $n=5$ for both experimental groups). Bars show means±s.d.

interval 0.804–1.043 L_0 s^{-1}) and 0.3560 L_0 s^{-1} for transverse muscles (95% confidence interval 0.2908–0.4414 L_0 s^{-1}). These velocities reflect not only the intrinsic characteristics of the arm muscle contractile machinery but also the presence of different amounts of fibers oriented in many directions.

Overall, these data show that transverse muscles have lower contraction and shortening velocities; this, in line with the isometric contraction dynamics and force–frequency relationship results, suggests that they behave as 'slow' muscles compared with longitudinal muscles.

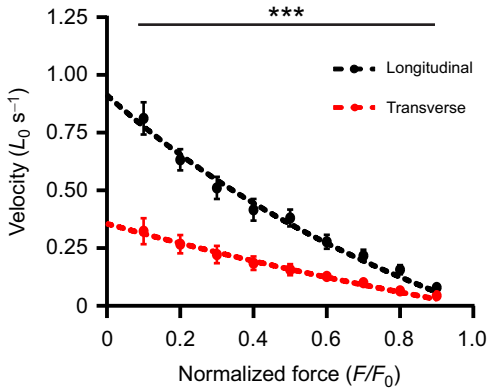

Fig. 6. Force–velocity relationship. The force and velocity were normalized for F_0 and L_0, respectively. Data are presented as means±s.e.m. The dashed lines represent the Hill fitting of the curves. Longitudinal muscles showed significantly higher shortening velocities than transverse muscles (mixed-effects model, $^{***}P<0.001$, $n=5$ for both experimental groups).

DISCUSSION

Motion control of hyper-redundant limbs is an important current topic, and several studies have been conducted in the last 10–20 years showing the adaptation of octopus arm motor control to various degrees of simplification strategies. These ultimately reduce the demands on the nervous system while still providing remarkable diversity of movements (Gutfreund et al., 1996; Sumbre et al., 2005, 2006, 2001; Zullo et al., 2011). In this study, we investigated the extent to which dynamic arm deformation can be facilitated by limb-embedded functional properties.

Octopus arms are capable of complex motions that are used in a wide repertoire of behaviors. These complex movements can be produced by a combination of four basic deformations: elongation, shortening, bending (orally, aborally, inward, outward) and torsion (clockwise and counterclockwise) (Kennedy et al., 2020). A fifth important component of arm motion is the arm 'stiffening' resulting from the co-contraction of longitudinal and transverse muscles. Stiffening allows the animal to use portions of the arms as dynamic skeletal elements in a variety of behaviors, from walking to reaching and fetching.

Given the cylindrical shape of the arm and its constant volume, longitudinal muscles undergo larger strain variations than transverse muscles. As a result, the lower stiffness of the longitudinal muscles may allow the accommodation of the larger range of strains experienced by these muscles during motions. In contrast, the

higher stiffness of the transverse muscles may be used to allow resistance to arm diameter increase, a crucial factor required to generate bending over longitudinal compression.

Interestingly, in these motions, arm deformation preferentially occurs within the first 2/3 of the arm, corresponding to the proximal–medial arm segments described in this work (Huffard et al., 2005; Levy et al., 2015). Hence, although continuous, the arm manifests a proximo-distal functional specialization. Interestingly, in our study, we found that the two main muscles making up the arm bulk, the longitudinal and transverse muscles, have different morphological aspect ratios along the arm. We showed that the longitudinal muscle is larger and the transverse muscle is smaller in the aboral medial–distal arm regions. Given the importance of the longitudinal muscles in bending, this might correspond to the highest rate of bend formation occurring in these arm segments (Kennedy et al., 2020). We also found that the aboral transverse diagonal extension of the transverse muscle is maximal at proximal–medial regions. This might be in line with the observation that arm elongation, which is driven by the decrease in diameter induced by transverse muscle contraction, occurs preferentially in the proximal region of the arm (Kennedy et al., 2020; Huffard et al., 2005; Levy et al., 2015). Thus, activation of muscles from different regions of the arm may produce different types of movements. Conversely, oblique muscles that support motions such as arm twisting, occurring along the entire arm length (Kennedy et al., 2020), manifest a uniform distribution throughout the arm.

Several examples of muscle functional specialization can be found in both vertebrates and invertebrates, where even different anatomical regions in single muscles may serve a variety of functions (Ahn et al., 2018; Ting and Chiel, 2017). For instance, in the cat hindlimb muscles, the biceps femoris is involved in slow walking, whereas the posterior regions are recruited during faster motions (Chanaud and Macpherson, 1991). Likewise, in the buccal retractor muscle of the invertebrate *Aplysia californica*, the anterior and posterior parts are activated and used differently during feeding behavior (McManus et al., 2014). These anatomical organizations can also be paralleled by differences in the muscle biomechanics.

This seems to be the case for the octopus arm, as we showed that the transverse and longitudinal muscles intrinsically differ in their active biomechanical properties. Specifically, we found that transverse muscles manifest slow activation properties and relaxation kinetics typical of skeletal slow-twitch muscles, such as the soleus (Hessel and Joumaa, 2019). They may thus be adapted to sustain strong and prolonged period of activity and to work as ‘postural’ muscles. Conversely, the longitudinal muscles show faster characteristics typical of skeletal fast-twitch muscles, such as the extensor digitorum longus (Hessel and Joumaa, 2019), which supports their involvement in finely tuned movements, such as bending and manipulation, typical of the octopus arms.

Interestingly, both transverse and longitudinal muscles show similarities in activation properties and relaxation/contraction kinetics to those of the transverse musculature of the squid arm, but not to the tentacle (see Table S1). However, we should consider that no information is currently available on the biomechanics of the squid longitudinal muscles. Similar to other cephalopod hydrostatic organs, the transverse and longitudinal muscles were able to produce significant fractions of their maximal force over a wide range of lengths (Milligan et al., 1997; Thompson et al., 2014), and they did not substantially differ in the active force–length relationships. We also showed that the maximal tetanic force of the transverse muscles was lower than that recorded in other cephalopod muscle limbs. This might be due to the presence in this type of muscle of a large amount of fibers oriented in many directions (including orthogonal fibers not contributing to the force estimated). Moreover, we cannot exclude the possibility that a variation in the protein of the contractile machinery might also exist and account, at least partially, for the differences observed. In order to elucidate this point, single muscle fiber force measurements and proteomic analysis of arm muscles should be carried out. Altogether, we suggest that the octopus arm muscles behave as slow or fast muscles based on their passive and active properties.

In line with what is shown in Di Clemente et al. (2021), transverse and longitudinal muscles also showed significant differences in their passive force component, which was significantly larger in transverse muscles. Passive forces in the arm muscles are due to the massive presence of coiled elastic fibers (see Fig. S5), arranged differently in the two muscles and supporting the arm passive response to deformations (Di Clemente et al., 2021). Compared with typical vertebrate muscles, the longitudinal and transverse muscles manifest passive properties similar to skeletal and cardiac muscles, respectively (Feher, 2012). Passive mechanical properties are major determinants of cardiac function and are due to the composition of titin, collagen and intermediate filaments (Emig et al., 2021; Granzier and Irving, 1995). In skeletal muscles, passive components contribute less to the total tension and are mainly due to the tendons and extracellular matrix. These not only work as elastic elements but, together with bones, also hold muscles to a resting length that is close to their optimal, at which the production of tension is maximized (Konow et al., 2012; Roberts, 2016).

Intuitively, this situation is significantly different for hydrostatic bodies. The complete absence of any internal or external rigid skeletal elements endows muscles with unprecedented freedom. In contrast, the presence of internal hydrostatic pressure may influence muscle contractile forces and response to deformation (Kier, 2020; Sleboda and Roberts, 2019).

Di Clemente et al. (2021) showed that intrinsic tensional stress within the arm causes transverse and longitudinal muscles to be held under different strain conditions in the arm at rest. Hence, they will operate on different regions of their force–length relationship, with transverse muscles closer to their L_0 and longitudinal muscles farther away from it, and they will produce different amounts of force when activated (Fig. 7). Thus, the same type of motor neuronal input reaching transverse or longitudinal muscles can induce different responses depending on the strain level. This allows the same muscle to become functionally different, thereby providing an intelligent mechanism to increase its flexibility in use.

What is the functional significance of this difference in operating length? Why should it be convenient to hold a muscle in a non-optimal length range? Perhaps we should consider the following: muscles have not evolved only to generate power but also to ‘stabilize’ posture, regulate the fine execution of movement and, in the case of hydrostatic limbs, support the structure through stiffening. This is achieved through both contractile and elastic elements of the muscle, the latter being very relevant in hydrostatic limbs, acting synergistically in the body musculature.

To illustrate this concept, we will dissect one exemplary octopus arm motion point by point: the arm extension. Arm extension starts with the formation of a bending point along the first 2/3 of the arm, preferentially in the lateral and aboral-up directions (Kennedy et al., 2020). The significant reduction in transverse elements at the oral side of the arm preferentially favors bend formation in this direction, thus allowing the suckers to be directly exposed to the probing environment. Bend production is due to the contraction of the

Journal of Experimental Biology (2022) 225, jeb243163. doi:10.1242/jeb.243163

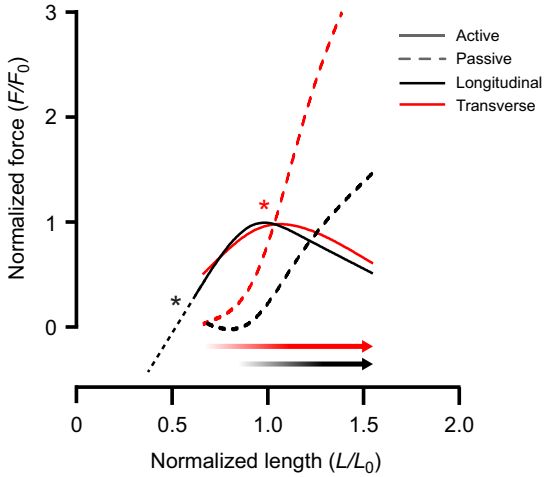

Fig. 7. Shift in muscle operating length in an intact arm. Spline fitting of passive and active force–length relationships for transverse and longitudinal muscles. Black and red asterisks indicate the operating points of transverse and longitudinal muscles in an arm at rest based on the tensional stress reported by Di Clemente et al. (2021). It is worth noting that the passive tension of the transverse muscle (red arrow) is greater at shorter lengths, while the longitudinal muscle passive tension begins to rise at values close to its L_0 (black arrow). Altogether, this suggests that although transverse and longitudinal muscles do not manifest major differences in their active force–length curves, their strain level allows them to work in different regions of their force–length curve and produce variable amounts of force.

transverse and longitudinal muscles on one side of the arm, with concomitant elongation of the longitudinal muscles on the opposite side. This would induce elastic forces of both transverse (on the bending site) and longitudinal (on the side opposite to bending) muscles to be 'released', hence reducing the energetic cost for bending.

Upon bend formation, arm extension is generated through gradual stiffening of the arm, which propels the bend towards the arm tip (Gutfreund et al., 1998, 1996; Sumbre et al., 2001). Arm stiffening is achieved through the co-contraction of the transverse and longitudinal muscles. During this process we can expect, based on the configuration of the passive elastic elements, transverse muscles to be 'favored' in contraction and longitudinal muscles to be 'disfavored', thus possibly producing a canceling effect of their elastic forces. Finally, and perhaps not least important, arm reconfiguration after extension (the arm returning to its resting state) might be reached, at reduced cost, simply by stopping muscle contraction, thus allowing for passive redistribution of strain along the arm. Notably, the possibility of generating stiffening in selective muscle layers of hydrostatic muscles also has profound implications for motor control strategies as stiffened muscles can be used as artificial 'skeletons' against which other muscles can act through contraction (Hooper, 2006; Kier, 2012).

Additionally, in soft tissue structures, the expansion or contraction of one muscle can significantly affect the surrounding muscles. For instance, changing the shape of one muscle can alter the mechanical advantage of other muscles, enhancing or reducing their ability to produce force (Novakovic et al., 2006). Therefore, the contribution of arm muscles to specific behaviors is the result of a fine interplay between their physiological properties, morphological arrangement and anatomical positioning, allowing muscles to move relative to one another and produce different motions.

The existence of arm regionalization, together with the muscle-specific biomechanical properties, represents an arm-embedded readily accessible system for a neural motor code to reconfigure the limb without the need for a complex feed-forward process. Thus, it may be an additional simplification strategy developed to further reduce the complexity of controlling highly flexible structures.

Conclusion

Here, we show that although continuous, octopus arms are endowed with a certain degree of regional specialization, where the arm muscles manifest different biomechanical properties. However, adaptation of arm muscle physiology is only part of a scenario in which muscle embedding and regionalization play an important role in the determination of muscle use during specific tasks. The type of motion produced by the arm is linked to the type of muscle activated, its initial state and the specific arm region involved.

Thus, to have a comprehensive understanding of octopus arm motor performances, muscle activation and biomechanical properties need to be interpreted in light of their embedding and anatomical organization within the arm. This consideration is particularly relevant in the field of bio-robotics, as it may provide important insights into both the construction and activation of artificial soft elements while leveraging their control architecture (Kang et al., 2016; Zullo et al., 2012).

Taken together, our results support the idea that cephalopods are distinguishable animals that have used simplification strategies, based on multifunctional design constraints, to control hyper-redundant limbs and bodies in a large variety of environmental niches (Hanlon and Messenger, 2018; Ponte et al., 2021). Thus, we can consider the octopus as an ensemble of well-coordinated effectors, from neural organization to body constraints.

Acknowledgements

We thank Benny Hochner for valuable discussions, Giacomo Pruzzo for technical assistance, Dr Marcello Ceppi for valuable statistical assistance and the animal care and maintenance facility of the IRCCS, San Martino Hospital of Genoa.

Competing interests

The authors declare no competing or financial interests.

Author contributions

Conceptualization: L.Z.; Methodology: A.D.C., F.M.; Software: A.D.C.; Formal analysis: A.D.C., F.M.; Investigation: L.Z., A.D.C., F.M.; Data curation: A.D.C., F.M.; Writing - original draft: L.Z., A.D.C.; Writing - review & editing: L.Z., A.D.C.; Supervision: L.Z.; Funding acquisition: L.Z.

Funding

This work was supported by the Seventh Framework Programme (OCTOPUS IP, Project Number FP7-231608), European Cooperation in Science and Technology (FA 1301 CephsInAction), and Office of Naval Research (award number N00014-21-1-2516).

References

Ahn, A., Konow, N., Tijs, C. and Biewener, A. (2018). Different segments within vertebrate muscles can operate on different regions of their force-length relationships. *Integr. Comp. Biol.* **58**. doi:10.1093/icb/icy040

Budelmann, B. (1978). *Octopus: Physiology and Behaviour of an Advanced Invertebrate* (ed. M. J. Wells). Chapman and Hall.

Burkholder, T. J. and Lieber, R. L. (2001). Sarcomere length operating range of vertebrate muscles during movement. *J. Exp. Biol.* **204**, 1529-1536. doi:10.1242/jeb.204.9.1529

Chanaud, C. and Macpherson, J. (1991). Functionally complex muscles of the cat hindlimb. III. Differential activation within biceps femoris during postural perturbations. Experimental brain research. Experimentelle Hirnforschung. *Expérimentation cérébrale* **85**, 271-80. doi:10.1007/bf00229406

Di Clemente, A., Maiole, F., Bornia, I. and Zullo, L. (2021). Beyond muscles: role of intramuscular connective tissue elasticity and passive stiffness in octopus arm muscle function. *J. Exp. Biol.* **224**, jeb242644. doi:10.1242/jeb.242644

Emig, R., Zgierski-Johnston, C. M., Timmermann, V., Taberner, A. J., Nash, M. P., Kohl, P. and Peyronnet, R. (2021). Passive myocardial

mechanical properties: meaning, measurement, models. *Biophys Rev* **13**, 587-610. doi:10.1007/s12551-021-00838-1

Feher, J. (2012). 5.7 - The Cellular Basis of Cardiac Contractility. In *Quantitative Human Physiology* (ed. J. Feher), pp. 477-485. Boston: Academic Press.

Fiorito, G., Affuso, A., Anderson, D. B., Basil, J., Bonnaud, L., Botta, G., Cole, A., D'Angelo, L., De Girolamo, P., Dennison, N. et al. (2014). Cephalopods in neuroscience: regulations, research and the 3Rs. *Invert. Neurosci.* **14**, 13-36. doi:10.1007/s10158-013-0165-x

Fiorito, G., Affuso, A., Basil, J., Cole, A., de Girolamo, P., D'angelo, L., Dickel, L., Gestal, C., Grasso, F., Kuba, M. et al. (2015). Guidelines for the care and welfare of cephalopods in research –A consensus based on an initiative by CephRes, FELASA and the boyd group. *Lab. Anim.* **49**, 1-90. doi:10.1177/0023677215580006

Fossati, S. M., Benfenati, F. Zullo, L. (2011). Morphological characterization of the Octopus vulgaris arm. *Vie Milieu* **61**, 197-201.

Granzier, H. L. and Irving, T. C. (1995). Passive tension in cardiac muscle: contribution of collagen, titin, microtubules, and intermediate filaments. *Biophys. J.* **68**, 1027-1044. doi:10.1016/S0006-3495(95)80278-X

Gutfreund, Y., Flash, T., Yarom, Y., Fiorito, G., Segev, I. and Hochner, B. (1996). Organization of octopus arm movements: a model system for studying the control of flexible arms. *J. Neurosci.* **16**, 7297-7307. doi:10.1523/JNEUROSCI.16-22-07297.1996

Gutfreund, Y., Flash, T., Fiorito, G. and Hochner, B. (1998). Patterns of arm muscle activation involved in octopus reaching movements. *J. Neurosci.* **18**, 5976-5987. doi:10.1523/JNEUROSCI.18-15-05976.1998

Gutnick, T., Byrne, R. A., Hochner, B. and Kuba, M. (2011). Octopus vulgaris uses visual information to determine the location of its arm. *Curr. Biol.* **21**, 460-462. doi:10.1016/j.cub.2011.01.052

Gutnick, T., Zullo, L., Hochner, B. and Kuba, M. J. (2020). Use of peripheral sensory information for central nervous control of arm movement by octopus vulgaris. *Curr. Biol.* **30**, 4322-4327.e3. doi:10.1016/j.cub.2020.08.037

Hanlon, R. and Messenger, J. (2018). *Cephalopod Behaviour*. Cambridge University Press.

Hessel, A. L. and Joumaa, V. (2019). Optimal length, calcium sensitivity and twitch characteristics of skeletal muscles from mdm mice with a deletion in N2A titin. *J. Exp. Biol.* **222**, jeb200840. doi:10.1242/jeb.200840

Hooper, S. L. (2006). Motor control: the importance of stiffness. *Curr. Biol.* **16**, R283-R285. doi:10.1016/j.cub.2006.03.045

Huffard, C. L., Boneka, F. and Full, R. J. (2005). Underwater bipedal locomotion by octopuses in disguise. *Science* **307**, 1927. doi:10.1126/science.1109616

Kang, R., Guglielmino, E., Zullo, L., Branson, D. T., Godage, I. and Caldwell, D. G. (2016). Embodiment design of soft continuum robots. *Adv. Mech. Eng.* **8**, 1687814016643302.

Kennedy, E. B. L., Buresch, K. C., Boinapally, P. and Hanlon, R. T. (2020). Octopus arms exhibit exceptional flexibility. *Sci. Rep.* **10**, 20872. doi:10.1038/s41598-020-77873-7

Kier, W. M. (2012). The diversity of hydrostatic skeletons. *J. Exp. Biol.* **215**, 1247-1257. doi:10.1242/jeb.056549

Kier, W. M. (2016). The musculature of coleoid cephalopod arms and tentacles. *Front. Cell Dev. Biol.* **4**, 10.

Kier, W. M. (2020). Muscle force is modulated by internal pressure. *Proc. Natl. Acad. Sci. USA* **117**, 2245-2247. doi:10.1073/pnas.1921726117

Kier, W. M. and Curtin, N. A. (2002). Fast muscle in squid (Loligo pealei): contractile properties of a specialized muscle fibre type. *J. Exp. Biol.* **205**, 1907-1916. doi:10.1242/jeb.205.13.1907

Kier, W. M. and Stella, M. P. (2007). The arrangement and function of octopus arm musculature and connective tissue. *J. Morphol.* **268**, 831-843. doi:10.1002/jmor.10548

Konow, N., Azizi, E. and Roberts, T. J. (2012). Muscle power attenuation by tendon during energy dissipation. *Proc. Biol. Sci.* **279**, 1108-1113.

Levy, G., Flash, T. and Hochner, B. (2015). Arm coordination in octopus crawling involves unique motor control strategies. *Curr. Biol.* **25**, 1195-1200. doi:10.1016/j.cub.2015.02.064

Maiole, F., Tedeschi, G., Candiani, S., Maragliano, L., Benfenati, F. and Zullo, L. (2019). Synapsins are expressed at neuronal and non-neuronal locations in Octopus vulgaris. *Sci. Rep.* **9**, 15430. doi:10.1038/s41598-019-51899-y

McManus, J., Lu, H., Cullins, M. and Chiel, H. (2014). Differential activation of an identified motor neuron and neuromodulation provide aplysia's retractor muscle an additional function. *J. Neurophysiol*. **112**. doi:10.1152/jn.00148.2014

Milligan, B., Curtin, N. and Bone, Q. (1997). Contractile properties of obliquely striated muscle from the mantle of squid (Alloteuthis subulata) and cuttlefish (Sepia officinalis). *J. Exp. Biol.* **200**, 2425-2436. doi:10.1242/jeb.200.18.2425

Novakovic, V., Sutton, G., Neustadter, D., Beer, R. and Chiel, H. (2006). Mechanical reconfiguration mediates swallowing and rejection in Aplysia californica. *J. Comp. Physiol. A* **192**. 857-70. doi:10.1007/s00359-006-0124-7

Ponte, G., Taite, M., Borrelli, L., Tarallo, A., Allcock, A. L. and Fiorito, G. (2021). Cerebrotypes in cephalopods: brain diversity and its correlation with species habits, life history, and physiological adaptations. *Front. Neuroanat.* **14**, 565109. doi:10.3389/fnana.2020.565109

Richter, J. N., Hochner, B. and Kuba, M. J. (2015). Octopus arm movements under constrained conditions: adaptation, modification and plasticity of motor primitives. *J. Exp. Biol.* **218**, 1069. doi:10.1242/jeb.115915

Roberts, T. J. (2016). Contribution of elastic tissues to the mechanics and energetics of muscle function during movement. *J. Exp. Biol.* **219**, 266-275. doi:10.1242/jeb.124446

Sleboda, D. A. and Roberts, T. J. (2019). Internal fluid pressure influences muscle contractile force. *Proc. Natl. Acad. Sci. USA* **117**, 1772-1778. doi:10.1073/pnas.1914433117

Sumbre, G., Fiorito, G., Flash, T. and Hochner, B. (2005). Neurobiology: motor control of flexible octopus arms. *Nature* **433**, 595-596. doi:10.1038/433595a

Sumbre, G., Fiorito, G., Flash, T. and Hochner, B. (2006). Octopuses use a human-like strategy to control precise point-to-point arm movements. *Curr. Biol.* **16**, 767-772. doi:10.1016/j.cub.2006.02.069

Sumbre, G., Gutfreund, Y., Fiorito, G., Flash, T. and Hochner, B. (2001). Control of octopus arm extension by a peripheral motor program. *Science* **293**, 1845-1848. doi:10.1126/science.1060976

Taylor, J. and Kier, W. (2003). Switching skeletons: hydrostatic support in molting crabs. *Science (New York, N.Y.)* **301**, 209-210. doi:10.1126/science.1085987

Thompson, J. T., Shelton, R. M. and Kier, W. M. (2014). The length-force behavior and operating length range of squid muscle vary as a function of position in the mantle wall. *J. Exp. Biol.* **217**, 2181-2192.

Ting, L. and Chiel, H. (2017). Muscle, biomechanics, and implications for neural control. *Fundamental Concepts and New Directions*. doi:10.1002/9781118873397.ch12

Uyeno, T. A. and Kier, W. M. (2005). Functional morphology of the cephalopod buccal mass: a novel joint type. *J. Morphol.* **264**, 211-222. doi:10.1002/jmor.10330

Wells, M. J. (1978). *Octopus: Physiology and Behaviour of an Advanced Invertebrate*. A Halsted Press book. Chapman and Hall.

Zullo, L. and Hochner, B. (2011). A new perspective on the organization of an invertebrate brain. *Commun. Integr. Biol.* **4**, 26-29. doi:10.4161/cib.13804

Zullo, L., Sumbre, G., Agnisola, C., Flash, T. and Hochner, B. (2009). Nonsomatotopic organization of the higher motor centers in octopus. *Curr. Biol.* **19**, 1632-1636. doi:10.1016/j.cub.2009.07.067

Zullo, L., Fossati, S. M. and Benfenati, F. (2011). Transmission of sensory responses in the peripheral nervous system of the arm of Octopus vulgaris. *Vie Milieu* **61**, 197-201.

Zullo, L., Chiappalone, M., Martinoia, S. and Benfenati, F. (2012). A "spike-based" grammar underlies directional modification in network connectivity: effect on bursting activity and implications for bio-hybrids systems. *PLoS One* **7**, e49299. doi:10.1371/journal.pone.0049299

Zullo, L., Fossati, S. M., Imperadore, P. and Nodl, M. T. (2017). Molecular determinants of cephalopod muscles and their implication in muscle regeneration. *Front. Cell Dev. Biol.* **5**, 53. doi:10.3389/fcell.2017.00053